ELSEVIER

European Journal of Mechanics A/Solids 21 (2002) 857–867

EUROPEAN JOURNAL OF MECHANICS A/SOLIDS

The flow-induced instability of long hanging pipes

Olivier Doaré, Emmanuel de Langre *

Département de Mécanique, LadHyX, École Polytechnique–CNRS, 91128 Palaiseau, France

Revised 14 August 2001; revised and accepted 4 February 2002

Abstract

The effect of increasing length on the stability of a hanging fluid-conveying pipe is investigated. Experiments show that there exists a critical length above which the flow velocity necessary to cause flutter becomes independent of the pipe length. The fluid-structure interaction is thus modelled by following the work of Bourrières and of Païdoussis. Computations using a standard Galerkin method confirm this evolution. A short pipe model is then considered, where gravity plays a negligible role. Transition between this short length model and the asymptotic situation is found to occur where a local stability criterion is satisfied at the upstream end of the pipe. For longer pipes, a model is proposed where the zone of stable waves is totally disregarded. Comparison of these models with experiments and computations show a good agreement over all ranges of mass ratios between the flowing fluid and the pipe.

Keywords: Pipe; Flutter; Stability; Wave; Gravity

1. Introduction

The fluid-conveying pipe is a dynamical system that has received considerable attention, partly because of its application in the oil and nuclear industries, partly because of its fascinating dynamical properties. It has thus been recognized as a model for a large variety of fluid-structure interaction problems, as extensively demonstrated by Païdoussis (1998). In a pioneering work Bourrières (1939) derived the linearized equations of motion of a beam-like structure conveying fluid and experimentally examined the flutter instability of a cantilevered pipe. This latter problem was subsequently solved by Gregory and Païdoussis (1966) and has since been referred to as the garden-hose instability. The instability of fluid-conveying pipes has then been extensively studied under a wide variety of flow conditions or mechanical characteristics. Excellent agreement has been found between experimental and predicted values of the flow velocity necessary for the onset of flutter in such systems. The particular case of a hanging cantilevered pipe was considered by Païdoussis (1970) who demonstrated the stabilizing effect of tension induced by gravity.

Comparatively little attention has been paid to the question of bending wave propagation in such beam-like structures with flow. Roth (1964) and Stein and Tobriner (1970) derived the stability conditions for harmonic waves. The stabilizing effect of tension on such waves has been analyzed by de Langre and Ouvrard (1999).

Clearly there is a need to establish a connection between analyses which consider the stability of finite length pipes, i.e. global approaches, and those which consider the stability of propagating waves along pipes of infinite length, i.e. local approaches. In the particular case of a pipe on an elastic foundation, Doaré and de Langre (2000, 2002) have shown that the local neutrality criterion is the global stability criterion for some sets of end-conditions. They have thus extended the criterion given by Kulikovskii (1966) for the relation between local and global stability of systems in which the length is increased.

The goal of the present paper is to study the instability properties of a hanging fluid conveying-pipe as its length is increased, and compare them with the local wave properties in the bulk of the pipe. A particularly interesting feature of this case is that

* Correspondence and reprints.
E-mail address: delangre@ladhyx.polytechnique.fr (E. de Langre).

0997-7538/02/$ – see front matter
PII: S0997-7538(02)01221-4

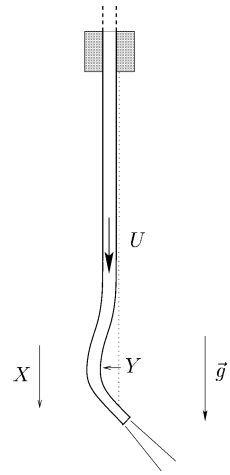

Fig. 1. Schematic view of the hanging fluid-conveying pipe.

local properties continuously vary along the pipe, the tension induced by gravity increasing from bottom to top. A preliminary set of results have been given in (de Langre et al., 2001) for the simpler case of low fluid mass where the system reduces to a problem of follower force.

The organisation of the paper is as follow: in Section 2, we present our experimental results of critical velocity for pipes of different lengths. In Section 3, the global critical velocity behavior is discussed in terms of local properties of waves along the pipe. In Section 4, a numerical investigation is used to extend the range of parameters.

2. Experiments

A first set of experiments on hanging pipes follows the same set-up as in Païdoussis (1970) but a wider range of dimensionless pipe length is explored. T.B. Benjamin made some exploratory experiments with very long hanging pipes in DAMTP, Cambridge, in the early 60s (Païdoussis, 2000) but drew no particular conclusion as to their asymptotic stability behavior. Two different pipes are used in the present study; the properties of these pipes are summarized in Table 1. The parameters used in this paper are the flexural rigidity EI, the internal diameter D, the mass per unit length of the pipe m, the mass per unit length of water in the pipe, M. The pipes are clamped at their upper end and their downstream end is free to move. Water flows from top to bottom. The fluid discharge is measured with a ball flowmeter.

As the flow rate is increased, the free pendulum oscillations of the pipe are initially strongly damped. Next, at the critical flow velocity, a flutter instability arises, and is characterized by limit cycle oscillations at a particular frequency (Bourrières, 1939). At the instability threshold, the flow rate Q and the oscillation frequency F of the limit cycle are measured. For pipes of small length, the oscillation frequency is measured using a stroboscope, while for longer pipes a chronometer is used.

Two different sets of non-dimensional parameters may be used. Assuming an average flow velocity $U = 4Q/\pi D^2$, Gregory and Païdoussis (1966) defined the non-dimensional mass ratio $\beta = M/(M+m)$, flow velocity, frequency and gravity as

$$u = UL\left(\frac{M}{EI}\right)^{1/2}, \qquad \Omega = 2\pi FL^2\left(\frac{M+m}{EI}\right)^{1/2}, \qquad \gamma = \frac{(M+m)L^3}{EI}g, \tag{1}$$

where L is the length of the pipe. These parameters have subsequently been used in most of the literature on fluid-conveying pipes (Païdoussis, 1970; Lottati and Kornecki, 1986; Doaré and de Langre, 2002). Since our goal is to investigate the behavior of

Table 1
Characteristics of the pipes used in experiments

Pipe	EI (N m^2)	D (m)	m (kg m^{-1})	M (kg m^{-1})	β
1	9.9E–4	4E–3	4.56E–2	1.26E–2	0.22
2	2.2E–4	4E–3	1.72E–2	1.26E–2	0.42
3	2E–3	5E–3	7.1E–2	1.96E–2	0.22

Pipes 1 and 2 refer to the experimental set up of Fig. 1, pipe 3 refers to that of Fig. 4.

cantilevered fluid-conveying pipes in the presence of gravity as the pipe-length is increased, we use a new set of non-dimensional parameters, where the characteristic length is not that of the pipe, but is related to the ratio between the flexural rigidity and the gravity force per unit length, namely

$$\eta = \left(\frac{EI}{(M+m)g} \right)^{1/3}. \tag{2}$$

This allows us to define a new set of parameters using η instead of L:

$$v = U\eta \left(\frac{M}{EI} \right)^{1/2}, \qquad \omega = 2\pi F \eta^2 \left(\frac{M+m}{EI} \right)^{1/2}, \qquad l = L/\eta. \tag{3}$$

We have the following relation between the two sets of dimensionless variables:

$$v = u\gamma^{-1/3}, \qquad \omega = \Omega\gamma^{-2/3}, \qquad l = \gamma^{1/3}. \tag{4}$$

Fig. 2 presents the experimental results for the critical velocity as a function of the length of the pipe for two different values of the mass ratio $\beta = 0.22$ and $\beta = 0.42$. The experimental results of Païdoussis (1970) for similar mass ratios are also plotted. In Fig. 2(a), the dimensionless parameters defined in (1) are used. Note that our study explores a much wider range of the

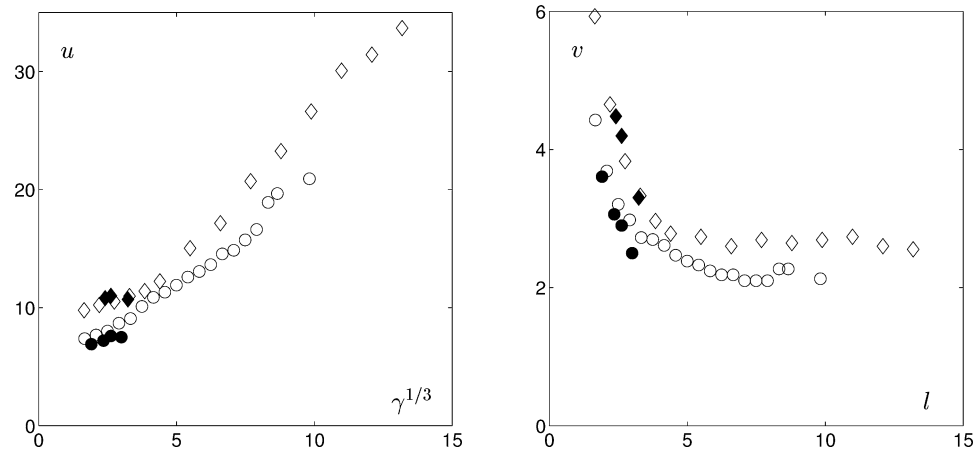

Fig. 2. Experimental critical flow velocity for the onset of flutter. (○), mass ratio $\beta = 0.22$; (◇), $\beta = 0.42$; (●) and (◆), experiments by Païdoussis (1970) for $\beta = 0.21$ and $\beta = 0.43$; (a), dimensionless velocity u based on the pipe length, Eq. (1); (b), dimensionless velocity v based on gravity, Eq. (3).

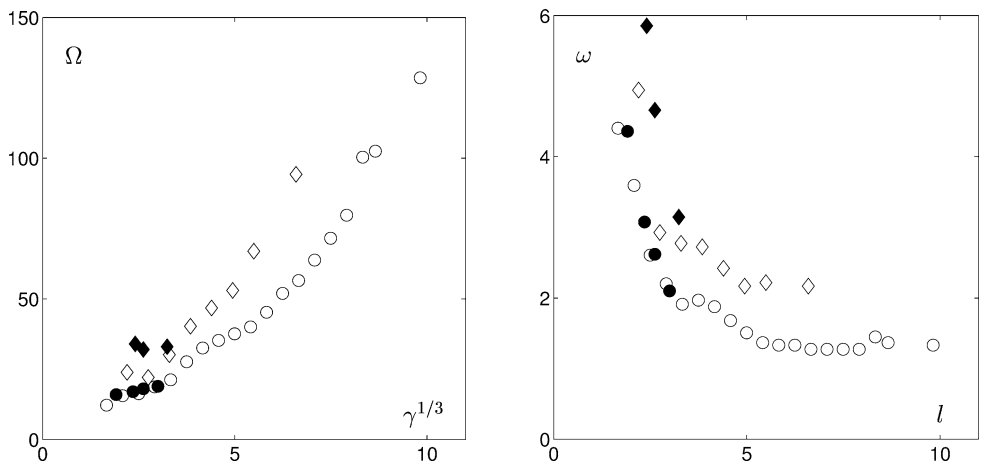

Fig. 3. Experimental critical frequency at the onset of flutter instability. (○), mass ratio $\beta = 0.22$; (◇), $\beta = 0.42$; (●) and (◆), experiments by Païdoussis (1970) for $\beta = 0.21$ and $\beta = 0.43$; (a), dimensionless frequency Ω based on the pipe length, Eq. (1); (b), dimensionless frequency ω based on gravity, Eq. (3).

gravity parameter γ than in previous work: $\gamma = 0{-}100$ in (Païdoussis, 1970), $\gamma = 0{-}1000$ for $\beta = 0.22$ and $\gamma = 0{-}2700$ for $\beta = 0.42$ in our experiments. Our data is in good agreement with those of previous work. Fig. 2(a) shows that, for a pipe of a given length, gravitational force increases stability, which is consistent with all observations of previous authors. Conversely, to explore the effect of the pipe length L at a given level of gravitational force, the same data need to be plotted in the (l, v) plane instead of the (γ, u) plane, the latter variables being both defined using L, Eq. (1). This is done in Fig. 2(b). We see that the critical velocity v first decreases as l is increased. After this, an asymptotic value is reached for longer pipes. This phenomenon is similar to that observed by Ni and Hansen (1978) in the case of flow-induced motions of flexible cables and cylinders with external flow. In a similar manner, the critical frequency is plotted in Fig. 3 as a function of the length of the pipe, with L as the reference length in Fig. 3(a), and with η as the reference length in Fig. 3(b). Again, the critical frequency ω is seen to reach an asymptotic value as the length is increased.

In order to characterize the shape of the oscillations at instability, a specific experimental setup is used, see Fig. 4. Following Borglund (1998), two pipes are attached symetrically to a long plastic sheet of 15 cm width and length $L = 1.15$ m, in such a manner that their natural bows are in opposite directions. This ensures straight pipes at rest, due to the mutual cancellation of the natural curvatures. Moreover, the movement at the onset of instability is in the (X, Y) plane due to the high rigidity of

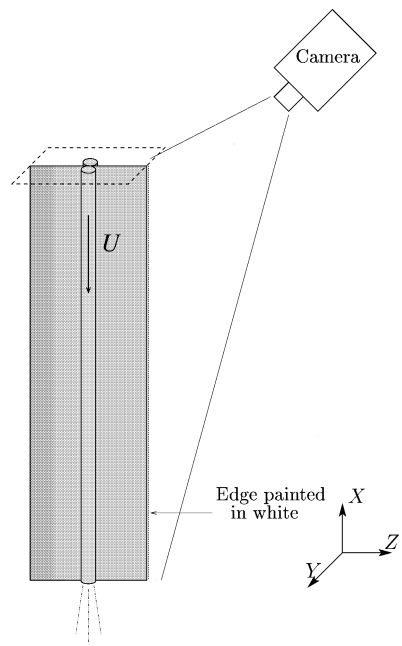

Fig. 4. Schematic view of the experimental set-up used to measure the pipe deflection.

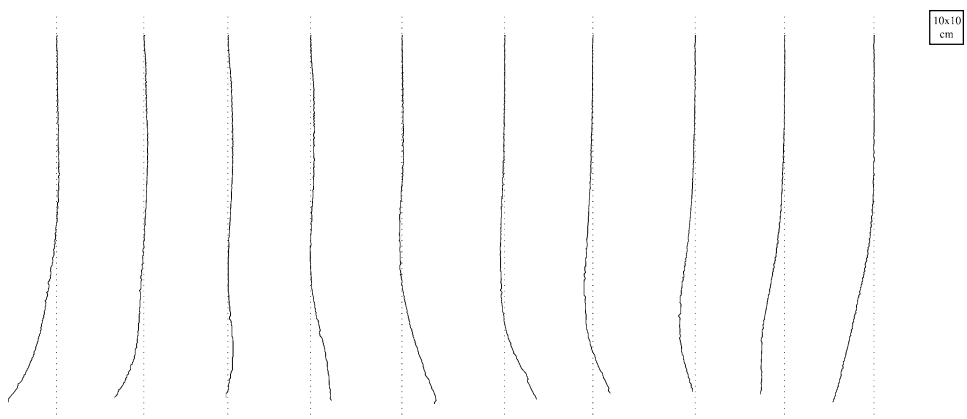

Fig. 5. Image sequence of the hanging pipe during one period of oscillation at instability, $\beta = 0.22$, $l = 8.4$, $v = 2.26$. The time step between each frame is $\Delta T = 0.8$ s.

the plastic sheet in the Z direction. Water flows through only one pipe. The characteristics of the system are summarized in Table 1 (pipe 3). A video camera is placed in the (Y, Z) plane at a small angle ($\sim 20°$) to the vertical axis. The whole system is painted in black except for one edge of the sheet which is painted in white. With appropriate light, the video image shows only the thin white edge of the sheet. Each image is then processed numerically to obtain the lateral deflection of each point of the pipe as a function of time. The time displacement of the pipe is deduced from the apparent motion of the line using the image of a reference grid placed in the plane of motion.

Fig. 5 shows a typical sequence of snapshots (after post-processing) equally spaced in time, over one period of oscillation for $v = 2.26$, $l = 8.4$. Note that the well-known garden-hose instability still exists for this long pipe ($l = 8.4$) but appears to be limited to its lower part. This observation will serve as a basis for the model developped in the next section.

3. Asymptotic behavior

In this section we establish a relation between the observed transition in the evolution of the critical velocity with length, and the existence of stable waves in the pipe. Two approximations are presented; one for short pipes and one for long pipes.

The linearized equation of motion governing the lateral in-plane deflection $Y(X, T)$ of a hanging fluid-conveying pipe of length L is, see (Païdoussis, 1998),

$$EI\frac{\partial^4 Y}{\partial X^4} + \left[MU^2 - g(M+m)(L-X)\right]\frac{\partial^2 Y}{\partial X^2} + g(M+m)\frac{\partial Y}{\partial X} + (2MU)\frac{\partial^2 Y}{\partial X \partial T} + (m+M)\frac{\partial^2 Y}{\partial T^2} = 0. \tag{5}$$

The third term $g(M+m)(L-X)$ is the tension that varies along the pipe. Its value is zero at the free downstream end and $(M+m)gL$ at the upstream clamped end. Using the reference length η defined in (2), we make the following change of variables:

$$x = X/\eta, \qquad y = Y/\eta, \qquad t = \left(EI/(M+m)\right)^{1/2} T/\eta^2, \tag{6}$$

so that Eq. (5) becomes, using the dimensionless parameters of (3),

$$\frac{\partial^4 y}{\partial x^4} + \left[v^2 - \chi\right]\frac{\partial^2 y}{\partial x^2} - \frac{\partial \chi}{\partial x}\frac{\partial y}{\partial x} + 2\sqrt{\beta}\, v\frac{\partial^2 y}{\partial x \partial t} + \frac{\partial^2 y}{\partial t^2} = 0, \tag{7}$$

where the dimensionless tension is

$$\chi = l - x. \tag{8}$$

The term $-\partial\chi/\partial x$ in Eq. (7) strictly equals unity. It is maintained here to bear in mind that this term arises from the varying tension, due to gravitational effects. The clamped upper end and free lower end require that

$$y|_{x=0} = \left.\frac{\partial y}{\partial x}\right|_{x=0} = \left.\frac{\partial^2 y}{\partial x^2}\right|_{x=l} = \left.\frac{\partial^3 y}{\partial x^3}\right|_{x=l} = 0. \tag{9}$$

It has been shown that for small lengths or equivalently low gravity, i.e. $\gamma \ll 1$, the critical velocity u, as defined in (1), is only a function of β (Païdoussis, 1970). Let $u_0(\beta)$ be the critical velocity for $\gamma = 0$. In terms of the velocity v, we may therefore expect a dependence on l for small lengths. Using Eq. (4), we express this as

$$v(\beta, l) = \frac{u_0(\beta)}{l}. \tag{10}$$

This will be referred to as the short pipe model.

Let us now analyze the behavior of the pipe in terms of wave propagation. At a given location in the pipe, say x, let us consider that the pipe is locally homogeneous in the x-direction and that the deflection of the pipe is of the form $y(x, t) = y_0 \exp[\mathrm{i}(kx - \omega t)]$. Substituting this into (7), we assume now that the tension does not vary locally, i.e. $\partial\chi/\partial x = 0$. The dispersion relation reads (Stein and Tobriner, 1970)

$$D(k, \omega, \beta; v, \chi) = k^4 - k^2\left(v^2 - \chi\right) + 2\sqrt{\beta}\, vk\omega - \omega^2 = 0. \tag{11}$$

Local properties of bending waves propagating along the pipe may now be analyzed in terms of wavenumber k and frequency ω. For any sinusoidal wave in the x-direction with a real wavenumber k, the corresponding complex frequencies given by Eq. (11) are

$$\omega(k; \beta, v, \chi) = k\left(\sqrt{\beta} \pm \sqrt{\beta v^2 + k^2 - v^2 + \chi}\right). \tag{12}$$

Local stability of the pipe is ensured if these complex frequencies are such that the displacement associated with any real wavenumber k remains finite in time. It is the case when $\mathrm{Im}[\omega(k)] \leqslant 0$, that is, using Eq. (12), when

$$\chi(x) > v^2(1-\beta). \tag{13}$$

The tension χ, given by Eq. (8), varies from 0 to l along the pipe, from bottom to top. Therefore, unstable waves always exist at the downstream end, provided that $v \neq 0$ and $\beta \neq 1$. We may now differentiate two situations depending on the parameters:

(a) if $l < v^2(1-\beta)$, every point of the pipe supports unstable waves, the criterion of Eq. (13) being violated for all x;
(b) if $l > v^2(1-\beta)$, two regions exist in the pipe, a lower region $l > x > l - v^2(1-\beta)$ of instability, and an upper region where the local stability criterion (13) is satisfied, $l - v^2(1-\beta) > x > 0$.

Transition between these two cases occurs at the critical position

$$l_c = v^2(1-\beta). \tag{14}$$

When the length l is larger than l_c, we conclude from the experimental results presented in Fig. 5 that the dynamics of the pipe is controlled by the unstable zone at the downstream end. Let us therefore consider a pipe of length $l = v^2(1-\beta)$ with constant tension

$$\chi = \frac{v^2(1-\beta)}{2}. \tag{15}$$

This is in fact the mean value of the tension in the full pipe problem; see Fig. 6. We consider this as an approximation for long hanging pipes. Its equation of motion reads, using (7) and (15):

$$\frac{\partial^4 y}{\partial x^4} + \left[(1+\beta)\frac{v^2}{2}\right]\frac{\partial^2 y}{\partial x^2} + 2\sqrt{\beta}\, v \frac{\partial^2 y}{\partial x \partial t} + \frac{\partial^2 y}{\partial t^2} = 0 \tag{16}$$

with the same boundary conditions as in Eq. (9). Defining $\beta_0 = 2\beta/(1+\beta)$ and $v_0 = v\sqrt{(1+\beta)/2}$, Eq. (16) becomes

$$\frac{\partial^4 y}{\partial x^4} + v_0^2 \frac{\partial^2 y}{\partial x^2} + 2\sqrt{\beta_0}\, v_0 \frac{\partial^2 y}{\partial x \partial t} + \frac{\partial^2 y}{\partial t^2} = 0, \tag{17}$$

where x varies from 0 to l_c. Using the dimensionless variables referring to the length $L_c = \eta l_c$, it reads

$$\frac{\partial^4 y}{\partial x^4} + u_0^2 \frac{\partial^2 y}{\partial x^2} + 2\sqrt{\beta_0}\, u_0 \frac{\partial^2 y}{\partial x \partial t} + \frac{\partial^2 y}{\partial t^2} = 0, \tag{18}$$

where x varies from 0 to 1. This is the equation of motion of a cantilevered pipe without tension or gravity, as originally solved by Gregory and Païdoussis (1966), leading to the well-known critical velocity function $u_0(\beta_0)$: We may therefore state that the critical velocity for our long pipe model reads:

$$v_\infty(\beta) = \left(\frac{u_0(\beta_0)}{1-\beta}\right)^{1/3}\left(\frac{2}{1+\beta}\right)^{1/6}. \tag{19}$$

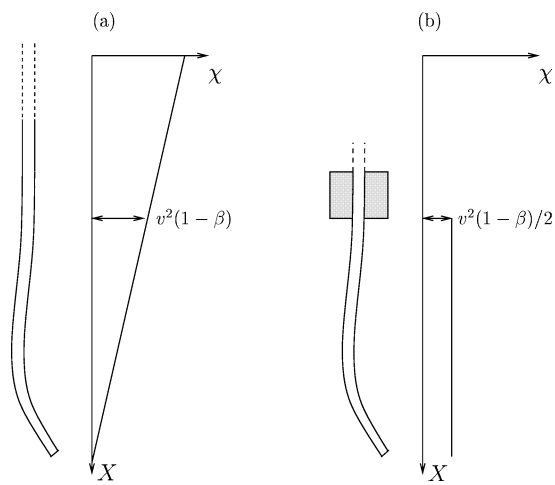

Fig. 6. Tension in the long pipe model, (a), semi-infinite pipe; (b), equivalent pipe of finite length.

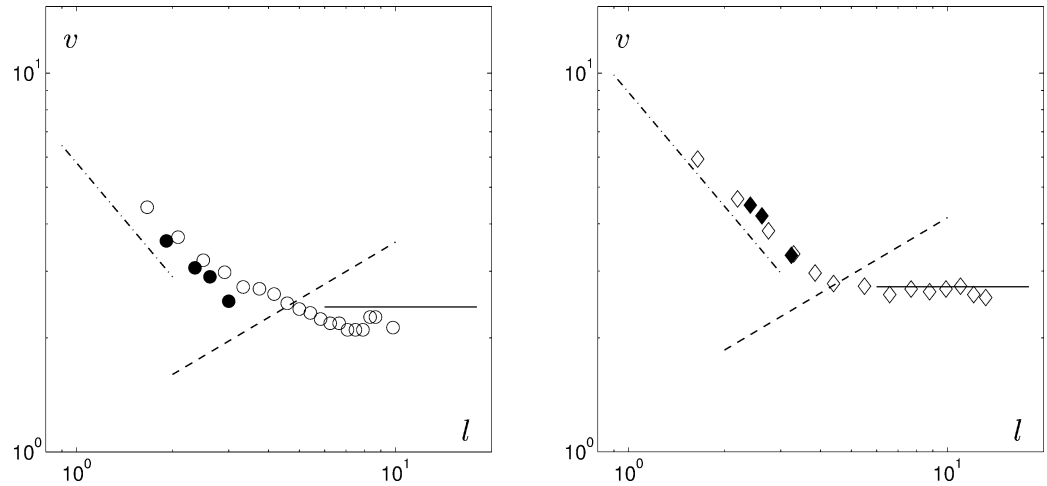

Fig. 7. Comparison between measured critical velocities and models, (○) and (◇), present experiments for $\beta = 0.22$ and $\beta = 0.42$, respectively; (●) and (◆), experiments by Païdoussis (1970) for $\beta = 0.21$ and $\beta = 0.43$; (– · – · –·), short pipe model, Eq. (10); (———), long pipe model, Eq. (19); (– – –), transition criterion based on local stability, Eq. (14).

The critical frequency for the long pipe model is similarly defined using Ω_0, the critical frequency at $u_0(\beta_0)$:

$$\omega_\infty(\beta) = \frac{\Omega_0(\beta_0)}{(1-\beta)^2 v_\infty^4(\beta)}. \tag{20}$$

In Fig. 7, the experimental critical velocity is plotted as a function of length for each pipe and is compared with

(a) the short pipe model, Eq. (10);
(b) the transition criterion based on local stability, Eq. (14); and
(c) the long pipe model, Eq. (19).

The experimental data is well described by the proposed models. Once a critical length is reached, all the dynamics of the system are therefore driven by the downstream end where unstable waves developp. Letting the pipe being longer that this critical length has thus no effect.

4. Effect of the mass ratio

The models described in the preceding section have been compared to experiments in the range of mass ratios $\beta = 0.22$ to $\beta = 0.42$. All previously published work on fluid-conveying pipes (see (Païdoussis, 1998)) have shown that the mass ratio has a strong and sometimes complex influence on instabilities. Yet, experiments on long hanging pipes with lower ($\beta < 0.2$) or higher ($\beta > 0.4$) mass ratios encounter practical difficulties. We therefore seek to extend the range of mass ratios through computational experiments. The Galerkin method used for this purpose is a straightforward extension of that used by other authors in large ranges of mass ratios for various problems of cantilevered pipes (Gregory and Païdoussis, 1966; Lottati and Kornecki, 1986; Doaré and de Langre, 2002).

Let us decompose the movement of the pipe in the truncated basis of the first n free modes of the pipe without flow or gravity:

$$y(x,t) = \sum_{j=1}^{n} \phi_j(x) q_j(t). \tag{21}$$

Substituting this into the equation of motion (7), multiplying by $\phi_k(x)$ and integrating over x from 0 to l, we obtain n coupled second-order evolution equations for $q_j(t)$ (Gregory and Païdoussis, 1966). In our computations, we have considered up to 80 modes to obtain, with acceptable accuracy, the eigenfrequencies of the pipe for the highest mass ratios. Assuming harmonic motion at frequency ω and transforming to a first order problem of dimension $2n$, we obtain an eigenvalue problem that yields the eigenfrequencies ω_p, $p = 1, 2n$, of the system. If one of these complex frequencies has a positive imaginary part, the system

is unstable. Let v be the critical velocity, at which one eigenfrequency enters the upper half-plane in the complex ω-plane. In Fig. 8, the computed critical velocity v is compared to the experimental data of Section 2 for $\beta = 0.22$ and $\beta = 0.42$. Clearly, the Galerkin approximation of Eq. (21) captures the dependance of the critical velocity on the length, even for long pipes. It is used to explore values of mass ratios outside the experimental range and, thereby, to evaluate our approximate solutions of the preceding sections. The nonmonotonic behavior of the computed curve is known to be a consequence of successive changes in the number of beam-mode contributions to the unstable mode. This has been already observed in the case of the fluid-conveying pipe without gravity (Gregory and Païdoussis, 1966). In Fig. 9, the computed critical velocities versus the length of the pipe are plotted for $\beta = 0.5$ and $\beta = 0.7$. Again, they are compared with the models for short and long pipes, Eqs. (10) and (19), and with the criterion for the transition between these two limit cases, Eq. (14). The models for long and short pipes seem to be good approximations of the behavior of the hanging pipe even at high values of β. The transition between short and long pipe models is seen to take place when the criterion of Eq. (14) is satisfied.

Finally, Fig. 10 compares the critical velocity of the long pipe model with the asymptotic critical velocities for long hanging pipes obtained experimentally and numerically for a large set of mass ratios. A similar comparison is made for frequencies in Fig. 11. From these two figures, the instability of the semi-infinite hanging pipe seems to be well described by the long pipe model. As to the critical length for transition between the short and long pipe models, two estimates are compared in Fig. 12. The first is the value of l where the critical velocity (computed or obtained experimentaly) crosses the local stability criterion,

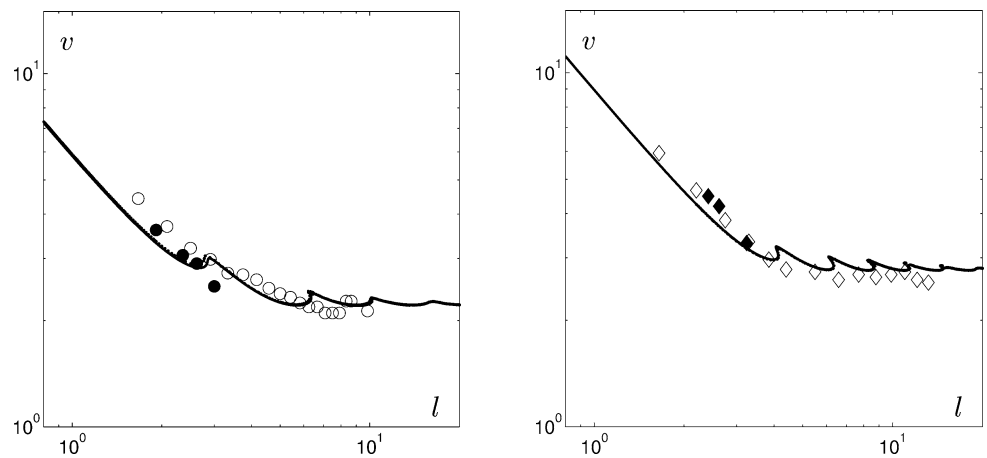

Fig. 8. Comparison between experimental and computed critical velocities. (○) and (◇), present experiments for $\beta = 0.22$ and $\beta = 0.42$; (●) and (◆), experiments by Païdoussis (1970) for $\beta = 0.21$ and $\beta = 0.43$; bold line, Galerkin computations.

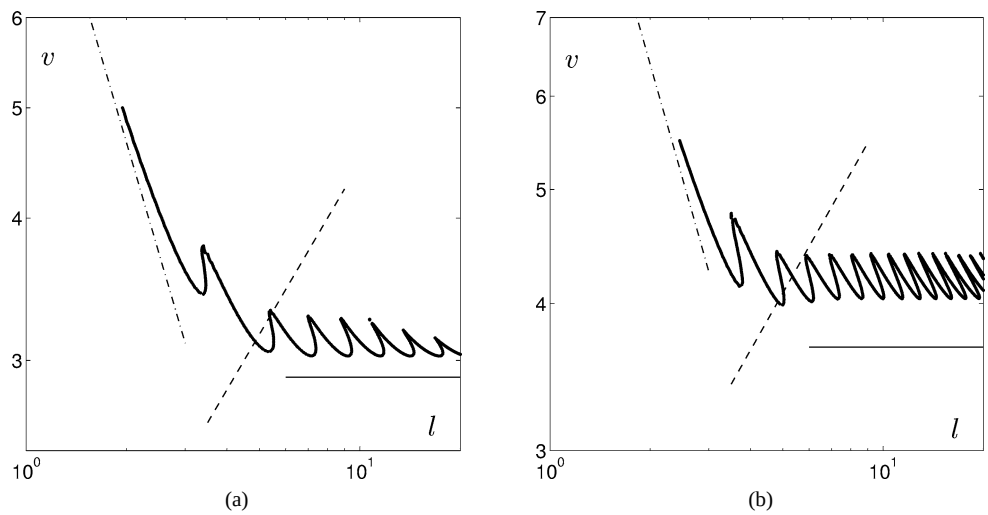

Fig. 9. Comparison between computed critical velocities and models; bold line, Galerkin computations; (– · – · –·), short pipe model, Eq. (10); (———), long pipe model, Eq. (19); (– – –), transition criterion based on local stability, Eq. (14); (a), $\beta = 0.5$; (b), $\beta = 0.7$.

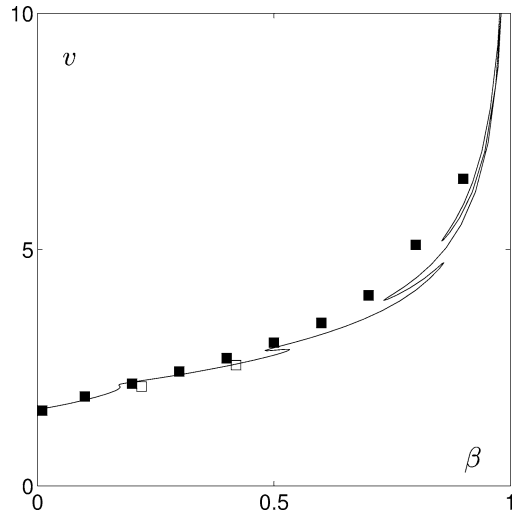

Fig. 10. Critical velocities for long hanging pipes, (■) computations; (□), experiments; (———), long pipe model, Eq. (19).

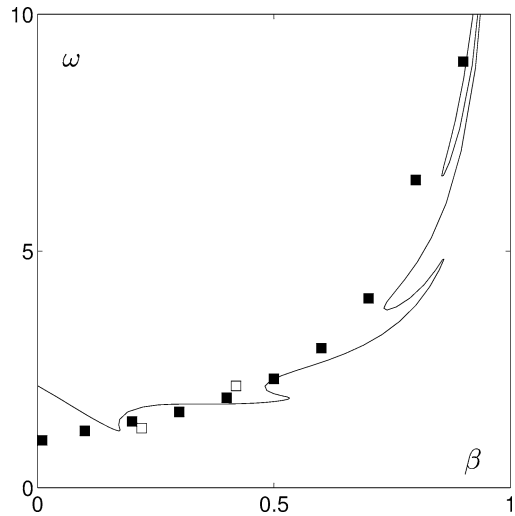

Fig. 11. Critical frequencies for long hanging pipes, (■) computations; (□), experiments; (———), long pipe model, Eq. (20).

Eq. (14). The second is the value of l where the short pipe solution, Eq. (10), equals the long pipe solution, Eq. (19). These two approximations of the transition length are in good agreement. It appears that transition occurs for a length which does not significantly depend on the mass ratio, typically $l \simeq 4$ that is, in dimensional variables,

$$L \simeq 4\left[\frac{EI}{(M+m)g}\right]^{1/3}. \tag{22}$$

Note that this is about twice the length that would make the standing pipe buckle under its own weight (Païdoussis, 1998).

5. Conclusion

In this paper we have investigated the effect that increasing the pipe length has on the stability of a hanging fluid-conveying pipe. We have observed in experiments that there exists a critical length above which the flow velocity needed to bring about flutter becomes independant of the pipe length. A similar effect has been observed with respect to the frequency of flutter. Computations using a standard Galerkin method have confirmed these observations and have shown that such an asymptotic behavior exists for all considered mass ratios.

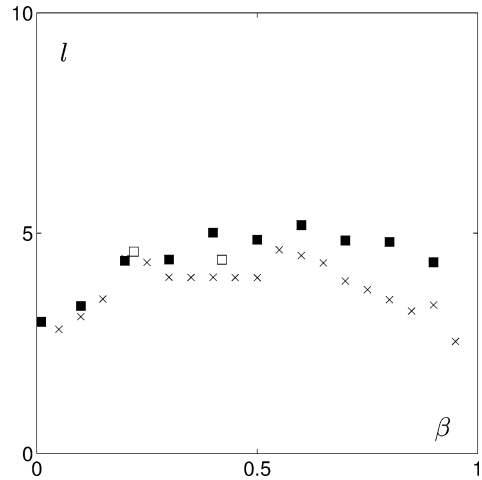

Fig. 12. Dimensionless length of transition between the short pipe and long pipe approximations, (×), length where the critical velocity of the short pipe model equals that of the long pipe model; (■), computations; (□), experiments.

When considering the stability of bending waves that develop in all locations along the pipe we have found that the asymptotic regime is reached when a region of wave stability exists in the upper part of the pipe. For long pipes, the additional upper length is highly tensioned and does not contribute to the development of instability, as observed experimentally. This analysis has been confirmed by a comparison between the characteristics of this asymptotic regime in terms of flow velocity and oscillation frequency and those from a simplified model when the upper stable region is neglected. Close agreement is found with experimental and numerical data. These results allow us to conclude that local wave properties are relevant to the analysis of the global behavior of hanging pipes.

Following similar analyses of semi-infinite systems with continuously varying local properties, it would seem natural to use a WKBJ-approach (Huerre and Rossi, 1998). Yet, considering the observed motion of the pipe, Fig. 5, it appears that the typical wavelength of instability is of the same order as the length of the unstable region, l_c. This violates the underlying assumptions of the WKBJ-approach. A link may also be sought between the frequency of oscillation of the semi-infinite pipe at instability and some local property such as the absolute frequency (see Huerre and Monkewitz (1990), Monkewitz et al. (1993)). This approach also fails, because the frequency selection is more related to a finite length effect, as shown by the present study.

Our results may help us to understand the behavior of other long systems submitted to non-conservative forces. The hanging beam with a follower force (i.e. a force whose direction varies as that of the beam axis) is a special case of the present analysis, which is obtained by setting $\beta = 0$, see (de Langre et al., 2001). Structures such as beams, plates, flags or shells submitted to axial flow with the upstream end fixed and the downstream end free are tensioned by the friction induced by flow (which has not been considered here as it is known to cancel out with pressure drop effects, see (Païdoussis, 1998)). These systems are therefore increasingly tensioned from the downstream to the upstream end and their behavior might be expected to become independent of the length as soon as a local stability criterion is satisfied at the upstream end. This is under current investigation.

References

Borglund, D., 1998. On the optimal design of pipes conveying fluids. Journal of Fluids and Structures 12, 353–365.

Bourrières, F.J., 1939. Sur un phénomène d'oscillation auto-entretenue en mécanique des fluides réels. Publications Scientifiques et Techniques du Ministère de l'Air 147.

Doaré, O., de Langre, E., 2000. Local and global instability of fluid-conveying cantilever pipes. In: Ziada, Staubli (Eds.), Flow Induced Vibration. Balkema, Rotterdam, pp. 349–354.

Doaré, O., de Langre, E., 2002. Local and global stability of fluid-conveying pipes on elastic foundations. Journal of Fluids and Structures 16 (1), 1–14.

Gregory, R.W., Païdoussis, M.P., 1966. Unstable oscillation of tubular cantilevers conveying fluids. I. Theory. Proccedings of the Royal Society London Series A 02936, 512–527.

Huerre, P., Monkewitz, P.A., 1990. Local and global instabilities in spatially developing flows. Annual Review of Fluid Mechanics 22, 473–537.

Huerre, P., Rossi, M., 1998. Hydrodynamic Instabilities in Open Flows. In: Godrèche, C., Manneville, P. (Eds.), Hydrodynamic and Nonlinear Instabilities. Cambridge University Press, Cambridge, pp. 81–294.

Kulikovskii, A.G., 1966. Cited in: Landau, L., Lifshitz, 1966. Physical Kinetics. In: Course of Theoretical Physics, Vol. 10. Pergamon Press, p. 281.

de Langre, E., Ouvrard, A.E., 1999. Absolute and convective bending instabilities in fluid-conveying pipes. Journal of Fluids and Structures 13, 663–680.

de Langre, E., Doaré, O., Pellet, F., 2001. Force suiveuse critique sur une colonne pesante semi-infinie: Modèle et expériences. Comptes Rendus de l'Académie des Sciences, Sér. IIb 329, 175–178.

Lottati, I., Kornecki, A., 1986. The effect of an elastic foundation and of dissipative forces on the stability of fluid-conveying pipes. Journal of Sound and Vibration 109, 327–338.

Monkewitz, P.A., Huerre, P., Chomaz, J.M., 1993. Global linear stability analysis of weakly non-parallel shear flows. Journal of Fluid Mechanics 251, 1–20.

Ni, C.C., Hansen, R.J., 1978. An experimental study of the flow-induced motions of a flexible cylinder in axial flow. Journal of Fluids Engineering 100, 389.

Païdoussis, M.P., 1970. Dynamics of tubular cantilevers conveying fluid. Journal Mechanical Engineering Science 12, 85–103.

Païdoussis, M.P., 1998. Fluid–Structure Interactions, Slender Structures and Axial Flow, Vol. I. Academic Press, London.

Païdoussis, M.P., 2000. Private communication.

Roth, W., 1964. Instabilität durchströmter Rohre. Ingenieur-Archiv 33, 236–263.

Stein, R.A., Tobriner, M.W., 1970. Vibration of pipes containing flowing fluids. ASME Journal of Applied Mechanics 37, 906–916.